GCOM-C/SGLI
Wild Fire detection and Fire Radiative Power (FRP) retrieval ATBD

Yukio Kurihara

JAXA/EORC

Ver. 0.0: Aug. 2020

1 Introduction

This document presents the technical background of the wildfire detection and the fire radiative power (FRP) retrieval for the Second Generation Global Imager (SGLI) onboard the Global Change Observation Mission-Climate (GCOM-C) satellite. Details on the GCOM mission, GCOM-C, and SGLI are described in Imaoka et al. [2010].

2 Data

Short wavelength infrared (SWIR) data at the SW3 (1.6 μm) and SW4 (2.9 μm) channels (Table 1) are used to detect hot spots and to determine the fire radiative power (FRP).

Table 1. SGLI channel specifications

Ch.**	λ	$\triangle\lambda$	L_{std}, L_{max}		SNR at L_{std}	IFOV
	$[nm]$	$[nm]$	$[W/m^2/sr/\mu m]$			$[m]$
VN1	380	10	60	240-241	624-675	250 / 1000
VN2	412	10	75	305-318	786-826	250 / 1000
VN3	443	10	64	457-467	487-531	250 / 1000
VN4	490	10	53	147-150	858-870	250 / 1000
VN5	530	20	41	361-364	457-522	250 / 1000
VN6	565	20	33	95-96	1027-1064	250 / 1000
VN7	673.5	10	23	69-70	988-1088	250 / 1000
VN8	673.5	20	25	213-217	537-564	250 / 1000
VN9	763	8	40	351-359	1592-1746	1000
VN10	868.5	20	8	37-38	470-510	250 / 1000
VN11	868.5	20	30	305-306	471-511	250 / 1000
P1	670	20	25	293	609	1000
P2	865	20	30	396	646	1000
SW1	1050	20	57	289.2	951.8	1000
SW2	1380	20	8	118.9	347.3	1000
SW3	1640	200	3	50.6	100.5	250 / 1000
SW4	2210	50	1.9	21.7	378.7	1000
Ch.	λ	$\triangle\lambda$	T_{std}, T_{max}		NE$\triangle$T at T_{std}	IFOV
	$[\mu m]$	$[\mu m]$	$[K]$			$[m]$
T1	10.8	0.7	300	340	0.08	250 / 500 / 1000
T2	12.0	0.7	300	340	0.13	250 / 500 / 1000

L: signal level, SNR: signal noise ratio, NE$\triangle$T: noise equivalent temperature difference, VN, P: non-polarization and polarization channel of VNR. SW, T: short-wavelength-infrared and thermal infrared channel of IRS.

3 Processing flow

SW3 and SW4 data (albedo) are translated into the radiances (hereinafter, denoted by L_{SW3} and L_{SW4}) at (a). Then, hot spots are detected through (b)−(e) and FRP is determined at (f). Finally, a report is generated at (g).

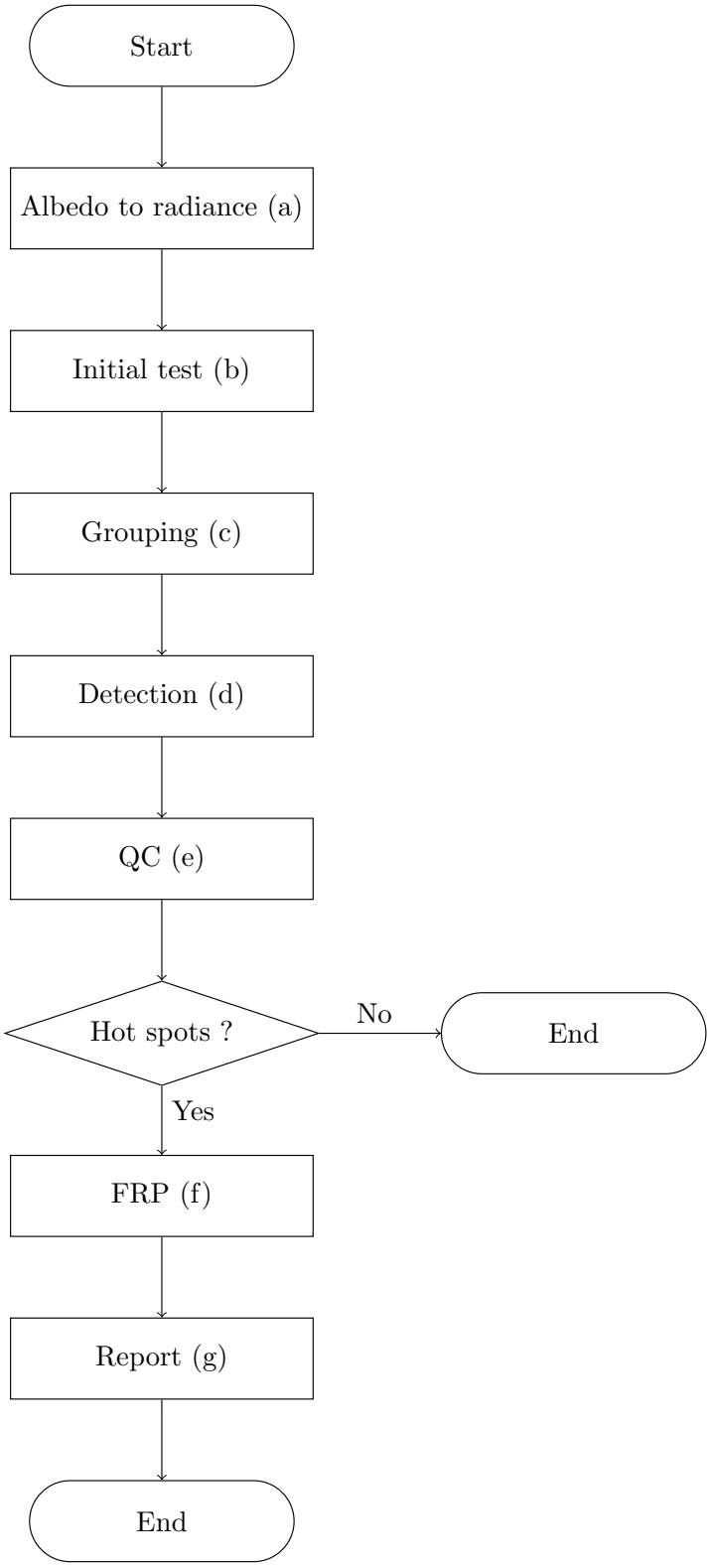

Figure 1

4 Algorithm

4.1 Hot spot detection

Pixels, where L_{SW3} and/or L_{SW4} are larger than the three times of the noise level ($3\sigma_e$), are selected at (b) in the flow. Then, selected pixels are divided into clusters at (c) by grouping the data spatially connected. Here, the method uses σ_e determined by L_{std}/SNR by using L_{std} and SNR in Table 1. The step (d) compares the maximum radiance in each cluster with the threshold of $4\sigma_e$. If the maximum radiance exceeds the threshold at SW3 or at SW4, all pixels in the cluster are detected as hot spots. Figure 2 shows the area fraction and the temperature range of the hot spot which is detectable by SW3 and SW4. Finally, a confidence level (Table 2) is decided for each hot spot at (e). Land cover types are quoted from the MODIS Land Cover Type Product. Detection frequency (Fig. 3) was generated at each 0.05×0.05-degree latitude-longitude grid by using hot spots detected for 2018 and 2019. Each threshold was arrived at empirically.

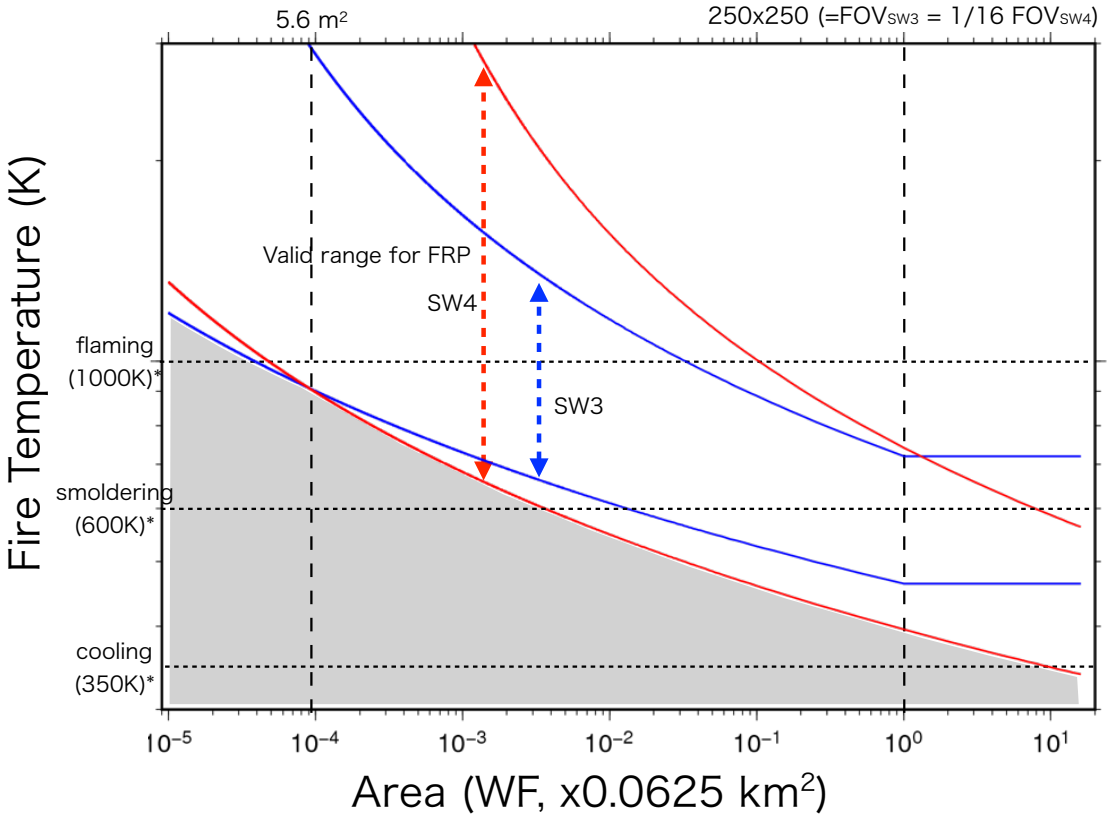

Figure 2. The fraction and temperature range of hot spots detectable with SW3 and SW4. Wildfire levels and those temperatures are quoted from Wooster et al. [2003]. The blue and red bottom lines denote the detection limit, and the top lines the saturation levels.

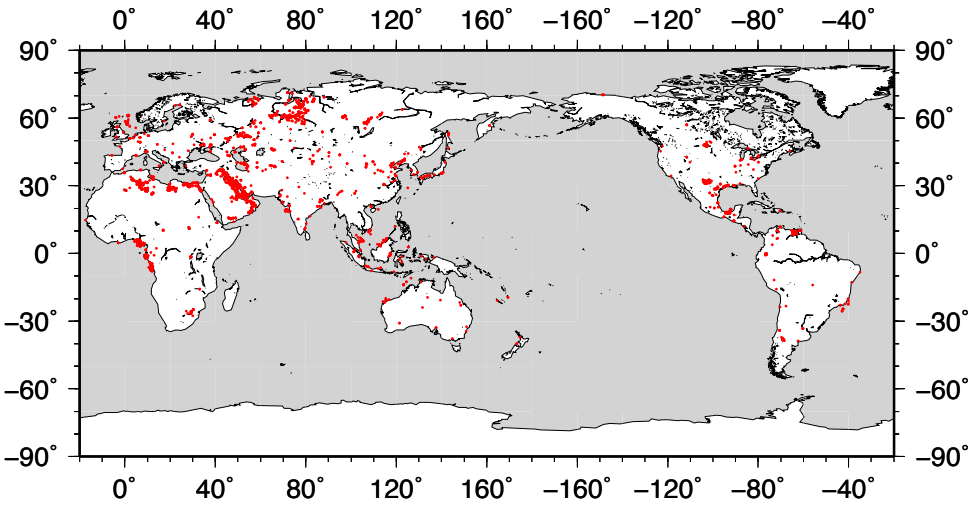

Figure 3. Frequently detected hot spots.

Table 2. Confidence level

Level	Description
1	L $< 8\sigma_e$ for land pixel, L $< 32\sigma_e$ for water pixel, non vegetated (snow, ice, barren), or detection frequency $> 50\%$
2	L $< 16\sigma_e$
3	L $< 32\sigma_e$
4	L $< 64\sigma_e$
5	L $\geqq 64\sigma_e$

4.2 FRP

Following Wooster et al. [2003], FRP is determined by performing the MIR radiance method on the SWIR data. The determination formula is

$$FRP_{MIR} = \left(\frac{\sigma \varepsilon_f}{a \varepsilon_{f,MIR}} \right) L_{f,MIR}. \tag{1}$$

Here, σ is the Stefan-Boltzmann constant, ε_f is the fire emissivity over all wavelengths, $\varepsilon_{f,MIR}$ is the fire emissivity for the MIR wavelength, a is a constant coefficient, and $L_{f,MIR}$ denotes the radiance of fire at MIR. In application of (1) to SWIR, ε_f and $\varepsilon_{f,MIR}$ were assumed to be 1.0, and $L_{f,MIR}$ was replaced by L_{SW3} or L_{SW4}; this was based on the assumption that SW3 and SW4 are insensitive to background temperatures. The coefficient was determined by using numerically simulated data (Table 3).

Table 3. FRP coefficients

	T_f (K)	σ/a	Quality flag
$SW3_1$	600	133.921	1
$SW3_2$	800	1639.2	2
$SW4_1$	650	100.254	3
$SW4_2$	700	65.9356	4
$SW4_3$	700	65.9356	5

		SW3		
		L< $3\sigma_e$	L<L_{max}	L≧L_{max}
SW4	L< $3\sigma_e$		$SW3_1$	
	L<L_{max}	$SW4_1$	$SW4_2$	$SW4_3$
	L≧L_{max}		$SW3_2$	

5 Report (Alert)

If there is any hot spot detected, an alert file is generated. The alert data consists of two parts: a header part and a data part. The header part is denoted by the '#' at the start of each record. The data acquisition and processed date and time and parameter names are provided in the header. The data part holds detected hot spots and determined FRPs in the comma-separated values (CSV) format. Table 4 shows the parameters described in the data part. The hot center indicates the hottest pixel in the fire cluster. Each fire cluster can be specified by gathering the hot spots associated with the same hot center. Note that the alert file is not generated if there is no hot spot detected.

Table 4. Data in the report

column	parameter	description
1	Hot-spot ID	
2	Year	
3	Month	
4	Day	
5	Time	hhmn in UTC
6	Latitude	
7	Longitude	
8	Area	Area factor ($1/cos(\theta_z)$)
9	Volcano	0: no volcano, 1: volcanos
10	Reliability	Table 2
11	FRP	Wm^{-2}
12	Quality flag	Table 3
13	Hot center (ID)	Hottest pixel in the cluster

6 Limitation

Because the reflected sunlight prevents detecting hot spots, the algorithm is limited only for nighttime. Note that the algorithm is disabled at high latitudes during the nights with the midnight sun.

7 Issues

The followings are the major issues with the wildfire detection and FRP retrieval method for SGLI data.

1. Hot spot detection for daytime is an issue that needs to be investigated in the future.
2. FRP determination is still tentative and needs to be improved in the future.

References

Imaoka, K., Kachi, M., Fujii, H., Murakami, H., Hori, M., Ono, A., Igarashi, T., Nakagawa, K., Oki, T., Honda, Y., and Shimoda, H. (2010). Global change observation mission (gcom) for monitoring carbon, water cycles, and climate change. Proceedings of the IEEE, 98(5):717–734.

Wooster, M., Zhukov, B., and Oertel, D. (2003). Fire radiative energy for quantitative study of biomass burning: derivation from the BIRD experimental satellite and comparison to MODIS fire products. Remote Sensing of Environment, 86(1):83 – 107.